Improvement of neutron sensitivity for lithium formate esr dosemeters: a monte carlo analysis

MC D'Oca[a,b]; G Collura[a,b], giorgio.collura01@unipa.it; C Gagliardo[c], cesare.gagliardo@unipa.it; A Bartolotta[a,b], antonio.bartolotta@unipa.it; M Romeo[a], mattia.romeo@community.unipa.it; F d'Errico[e,f]; M Marrale[a,b,d,*], maurizio.marrale@unipa.it

[a]Department of<<Query: Please check the spelling and accuracy of all author names and affiliations, particularly for any of your coauthors. Please also check that author surnames are correctly identified with a pink background. This is to ensure that forenames and surnames are tagged correctly for online indexing. {\bfseries Incorrect names and affiliations may lead to an author not being credited for their work by funders, institutions, or other third parties.} Ans: **maurizio.marrale@unipa.it:** We checked the name and affiliations of all authors. OK>><<Query: There is a charge of \pounds350, \euro525 or $600 per print colour figure. Please confirm if you are willing to pay the charge. There are no charges for publishing colour figures online only. Ans: **maurizio.marrale@unipa.it:** We want to publish color figure online only. So we are not willing to pay the charge.>><<Query: If your manuscript has figures or text from other sources, please ensure you have permission from the copyright holder. For any questions about permissions contact jnls.author.support@oup.com. Ans: **maurizio.marrale@unipa.it:** The manuscript has not figure or text from other sources.>><<Query: Please check that funding is recorded in a separate funding section if applicable. Use the full official names of any funding bodies, and include any grant numbers. Ans: **maurizio.marrale@unipa.it:** The funding section is ok.>><<Query: You may need to include a "conflict of interest" section. This would cover any situations that might raise any questions of bias in your work and in your article's conclusions, implications, or opinions. Please see here https://academic.oup.com/journals/pages/authors/authors_faqs/conflicts_of_interest. Ans: **maurizio.marrale@unipa.it:** All authors declare that they have no conflicts of interest.>><<Query: Journal policy requires authors to provide a data availability statement in their manuscript. Please confirm that this statement is included in your manuscript and that any required links or identifiers for your data are present in the manuscript as described or provide edits with the required information. Ans: **maurizio.marrale@unipa.it:** Data available on request from M. Marrale.>> Physics and Chemistry 'Emilio Segrè', University of Palermo, Viale delle Scienze, Ed.18, I-90128 Palermo, Italy

[b]Istituto<<Query: As per style, first and last names must be given in full. Please check and confirm. Ans: **maurizio.marrale@unipa.it:** Please find below the first and last names of all authors:Maria Cristina D'OcaGiorgio ColluraCesare GagliardoAntonio BartolottaMattia RomeoFrancesco d'ErricoMaurizio Marrale>> Nazionale di Fisica Nucleare (INFN), Catania Division, Via Santa Sofia, 64, ~~I-~~95123 Catania, Italy

[c]Biomedicine, Neuroscience and Advanced Diagnostics, University of Palermo, 90127, Palermo, Italy<<Query: Please provide postal code for affiliation 3. Ans: **maurizio.marrale@unipa.it:** We have added this information.>>

[d]ATeN Center, University of Palermo, Viale delle Scienze, Edificio 18, 90128 Palermo, Italy

[e]Dipartimento di Ingegneria Civile e Industriale, Università di Pisa, Largo Lucio Lazzarino, 2 56126 Pisa, Italy

[f]Magnetic Resonance Research Center, School of Medicine of Yale, 300 Cedar Street, PO Box 208043, New Haven, CT 06520-8043, USA

[*]Corresponding author: maurizio.marrale@unipa.it

Preprint submitted to Radiation Protection Dosimetry 14 November 2022

Abstract

This work presents the computational analysis of the sensitivity improvements that could be achieved in lithium formate monohydrate (LFM) electron paramagnetic resonance (EPR) dosemeters exposed to neutron beams. Monte Carlo (MC) simulations were performed on LFM pellets exposed to neutron beams with different energy spectra at various depths inside a water phantom. Various computations were carried out by considering different enrichments of ^{6}Li inside the LFM matrix as well as addition of different amounts of gadolinium oxide inside the pellet blend. The energy released per unit mass was calculated with the aim of predicting the increase in dose achievable by the addition of sensitizers inside the pellets. As expected, a larger amount of ^{6}Li induces an increase of energy released because of the charged secondary particles (i.e. ^{3}H ions and α-particles) produced after neutron capture. For small depths in water phantom and low-energy neutron spectra the dose increase due to ^{6}Li enrichment is high (more than three orders of magnitude with respect to the case of with ^{7}Li). In case of epithermal neutron beams the energy released in ^{6}Li-enriched LFM compound is smaller but larger than in the case of fast neutron beams. On the other hand, the computational analysis evidenced that gadolinium is less effective than ^{6}Li in improving neutron sensitivity of the LFM pellets. Discussion based on the features of MC transport code is provided. This result suggests that ^{6}Li enrichment of LFM dosemeters would be more effective for neutron sensitivity improvement and these EPR dosemeters could be tested for dosimetric applications in Neutron Capture Therapy.

Introduction

Neutron Capture Therapy (NCT) is a specific radiation therapy characterised by a biological targeting of cancer at the cellular level. This advanced therapy combines an initial introduction and accumulation of nuclei with high neutron cross section (such as ^{10}B or ^{157}Gd) inside the tumour cells with a following irradiation with thermal neutrons. The ^{10}B or ^{157}Gd nuclei, when hit by thermal neutrons, undergo nuclear reactions where secondary charged particles (such as alpha particles, recoiling ^{7}Li nuclei or Auger electrons) with short subcellular range are released and are able to kill the tumour cells selectively[1–3]. Recently, the development of accelerator-based systems for the neutron beams has given an important impulse to the spread of the experimental research in NCT. One key element for the success of this therapy is the precise and accurate characterisation of the mixed (neutron,γ) field used. Therefore, reliable dosimetric measurements are needed in order to quantify the various (neutron and photon) components of the mixed beam and to improve the therapy. Various dosimetric systems are used for radiation detection such as ionisation chambers[3, 4], semiconductor detectors[5, 6], thermoluminescence (TLD) and optically stimulated luminescence dosemeters (OSL)[7–14], multifoil neutron activation spectrometry[3, 15] and gel dosimetry[16–22]. Each technique has its advantages and disadvantages[23].

Dosimetry through electron paramagnetic resonance (EPR) has aroused large interest in the last years. This technique can detect the paramagnetic centres (such as free radicals and point defects) produced

after exposure to ionising radiations. EPR dosimetry with alanine ($C_3H_7O_2N$) samples has been recognised as reference standard for dose measurements[24–43]. However, recently, new materials were analysed for larger sensitivity than alanine such as ammonium tartrate, ammonium formate, taurine, potassium tartrate hemihydrate, dithionates, phenols, strontium carbonate, sodium tartrate dehydrate and strontium sulphate, clear fused quartz, glasses and some others[31, 44–69].

One compound that is very promising is the lithium formate monohydrate (LFM) which is more sensitive than alanine because of its narrower EPR spectrum, tissue-equivalence, good signal stability and response also for kV photon beams [44, 70–78].

In this work, a Monte Carlo simulation analysis was carried out with the aim of predicting the EPR response of LFM dosemeters with increased ^{6}Li abundance or after addition of gadolinium exposed to neutrons beams for possible dosimetric applications in NCT. In particular, the energy released in these LFM pellets with ^{6} Li or Gd exposed to neutron beams with composite energy spectra and under different irradiation set-ups.

Monte carlo simulation

Irradiation set-up

Monte Carlo N-Particle–MCNP5[79] radiation transport code was used to estimate the average amount of energy deposition per unit mass into lithium formate dosemeters enriched with ^{6}Li or added with gadolinium oxide. The irradiation set-up adopted was analogous to that used in previous works[42, 52, 54, 80] with the axial system symmetry (see for example Figure 1 of the article[54]). The LFM samples and the dosemeter holder are cylindrical (diameter = 1 cm) and coaxial. The dosemeters are placed inside a holder composed of two water layers (one above the dosemeter and the other below). To simulate measurements at various water depths from surface the measurements of pellets were carried out by setting a water layer (whose thickness was varied from 1.0 up to 10 cm) between the dosemeter and the neutron source. The computational analyses with ^{6}Li-enriched dosemeters were carried out by varying the isotopic abundance of ^{6}Li inside the samples. ^{6}Li/Li ratio ranges from 0% (for samples containing only the ^{7}Li isotope) up to 100% (for samples containing only the ^{6}Li isotope). Lithium with natural isotopic abundance and gadolinium oxide (Gd_2O_3) as additive were considered in the case of dosemeters with gadolinium. Gadolinium oxide, inserted as thin layers 100 μm thick, was placed between layers of lithium formate compound. The amount of gadolinium oxide inside the samples ranged between 0 and 75% of the total sample mass. As the gadolinium content increases the number of gadolinium oxide layers inside the dosemeter increases as well as the content of lithium formate decreases correspondingly.

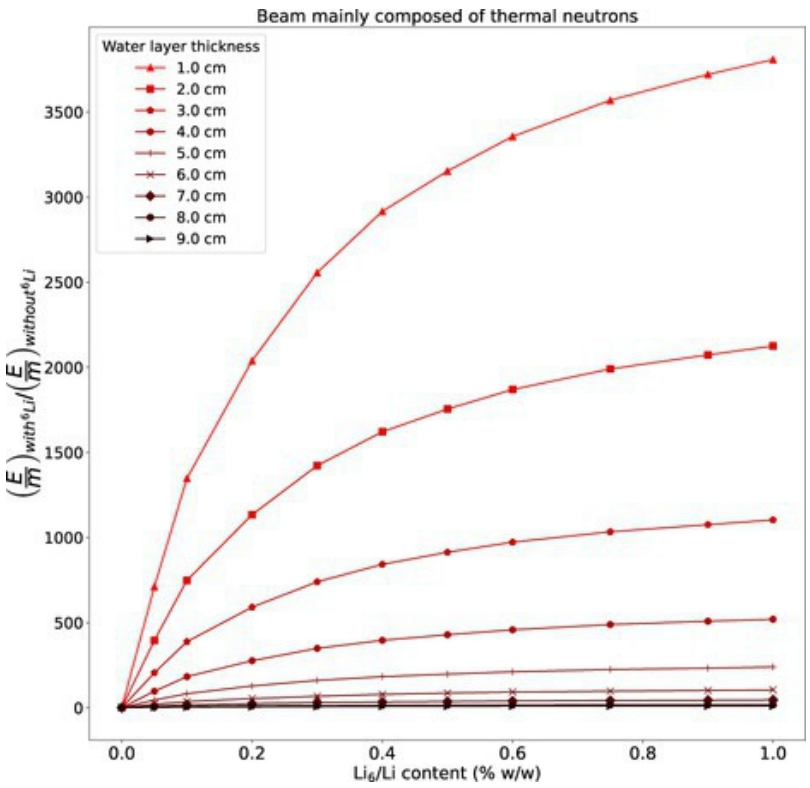

Figure 1 Energy released per unit mass with varying ^{6}Li content inside the sample for various thicknesses of the water layer above the dosemeter. In this case the neutron beam is mainly composed of thermal neutrons. The values are normalised to the values without ^{6}Li.

Neutron source

A disc-shaped neutron source, coaxial with z-axis and placed 20 cm from the bottom of the dosemeter, was considered and three neutron spectra with different energy composition were simulated. More details are provided in Table 1: the first spectrum is mainly composed of thermal neutrons, the second one is a main epithermal neutron and the third one is primarily composed of a fast neutron component.

Table 1 Energy neutron spectra used for Monte Carlo simulation.

	Energy range (eV)			
	0–0.1	**0.1–0.4**	**0.4–10^4**	**0.4–10^4**
Spectrum A	70%	22%	7%	1%
Spectrum B	1%	22%	70%	7%
Spectrum C	1%	7%	22%	70%

Results

In Figure 1 the results of the MC simulations related to the energy released inside lithium formate irradiated

with a mainly thermal neutron beam (Spectrum A) are reported. The values of the energy released per unit mass (which is an estimate of the absorbed dose) are shown with increasing the isotopic abundance of ^{6}Li inside the samples. The values are normalised to the values without ^{6}Li, i.e. the ratio $\left(\frac{E}{m}\right)_{with\ ^{6}Li} / \left(\frac{E}{m}\right)_{without\ ^{6}Li}$ is shown. Various calculations were performed to simulate irradiations at different depths in a water phantom irradiation.

As expected, the absorbed dose as well as neutron sensitivity increases as the ^{6}Li/Li ratio increases. This was expected because ^{6}Li nuclei have high thermal neutron capture of (i.e. $\sigma \approx 940$ barns) and the secondary charged particles (i.e. ^{3}H and α particle) produced after neutron capture are assumed to deposit energy locally in the dosemeter layer. The absorbed dose with ^{6}Li/Li = 100% is more than 3500 times larger than without ^{6}Li. Considering the case of Li natural isotopic abundance as reference and dividing the dose values by that absorbed by pellets with a Li natural isotopic abundance, a maximum dose increases larger than a factor 2.5 was observed. This means that large sensitivity improvements are observed for small ^{6}Li contents, with a sensitivity increase of >1000 when ^{6}Li/Li passes from 0 to 7.5% (that is, the ^{6}Li abundance in natural lithium), whereas at higher ^{6}Li contents the energy release enhancement is less evident. It is interesting to note that experimental EPR measurements performed on natural-Li and ^{6}Li-enriched lithium formate dosemeters exposed to a mainly thermal neutron beams have shown that the ^{6}Li-enriched dosemeters have a sensitivity 2.5 times larger than natural-Li pellets[78]. However, differences between the results reported in Lund *et al.*[78] and MC simulations here presented should be underlined. The pellets were experimentally irradiated to a mixed neutron-gamma field, whereas the MC analyses are performed considering only neutrons as incident particles (even though the secondary photons produced during neutron transport are considered). Furthermore, MC simulations assume that energies of secondary ^{3}H and α particles are deposited locally in the dosemeter layer and do not consider effects related to possible local electron–hole recombination and cluster formation. Nevertheless, these results show that, even though MC simulations do not take into account the phenomena of recombination sand saturations of free radicals which influence the EPR response of dosemeters, the computation analysis here performed is able to provide an estimate of response improvement due to ^{6}Li content inside the pellets.

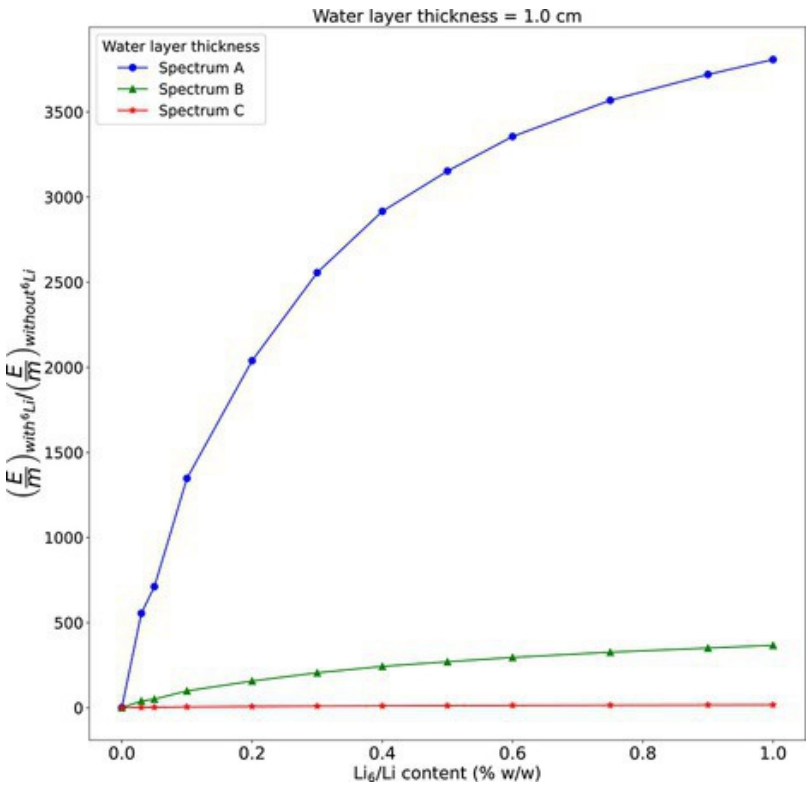

Figure 2 Comparison of energy released per unit mass for lithium formate samples exposed with different neutron spectra ('Spectrum A': mainly thermal neutron beam, 'Spectrum B': mainly epithermal neutron beam, 'Spectrum C': mainly fast neutron beam). The values are normalised to the values without ^{6}Li. The water layer above the pellet is 1 cm thick.

Figure 1 shows that the energy released inside the LFM layer decreases with increase in the thickness of the upper water layer because of the attenuation of the incoming beam inside this layer. The enhancement decreases with increase in the thickness of the water layer above the dosemeter (i.e. as the depth at which it is placed increases) and this is due to the fact that the thermal neutron component decreases with the depth. Variations of neutron energy spectra occur with a reduction of the thermal neutron component since the number of epithermal neutrons which are thermalized does not compensate for the thermal neutron losses. This reduces the signal enhancement due to ^{6}Li presence. These trends also provide information about the ability of these neutron beams to penetrate in water and release energy in depth and this could be useful for treatment planning with these neutron beams.

Figure 2 reports the comparison of the Monte Carlo results for lithium formate irradiated with neutron beams characterised by various energy spectra. In this case the thickness of the water layer above the dosemeter is 1 cm. For all neutron spectra considered the energy released increases with the ^{6}Li content. Furthermore, the absorbed dose decreases with increasing the average energy of the neutron beam and this is because ^{6}Li nucleus presents a very high neutron capture cross section for thermal energies, whereas the cross section is smaller for epithermal neutrons and much smaller for fast neutrons. If the energy released for 'Spectrum A' beam is considered as reference, the absorbed dose is about three times smaller for the 'Spectrum B' beam and about eight times smaller for the 'Spectrum C' beam.

The other target of this work is the investigation of the effects on neutron sensitivity related to the addition of

gadolinium oxide. Figure 3 shows the energy released per unit mass with increase in the gadolinium oxide concentration inside the dosemeters when the beams is mainly composed of thermal neutrons. The lithium present inside the LFM layers has natural isotopic abundance.

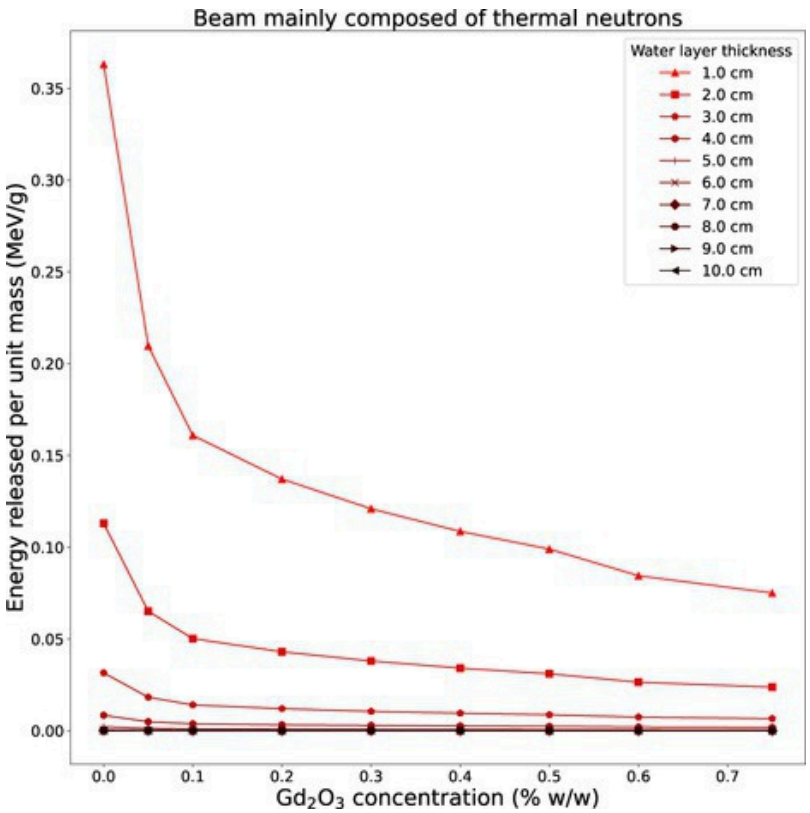

Figure 3 Energy released per unit mass with varying Gd_2O_3 content inside the sample for various thickness of the water layer above the dosemeter. In this case the neutron beam is mainly composed of thermal neutrons.

The trend observed decreases with the concentration of Gd_2O_3 inside the pellet. The absorbed dose is decreased to about 30% of its maximum value for Gd_2O_3 concentration of 75%. To explain this result some details about the MC computations should be considered. First, MCNP5 does not consider the transport of the secondary charged heavy particles (i.e. ^3H and α particle) released after neutron capture by ^6Li nuclei but assumes that energies released after the interaction are deposited locally in the place where the neutron capture occurs[(79)]. Since the Li nuclei are only present inside the dosemeter layer, this implies that the energy released after neutron capture by ^6Li is totally absorbed by the LFM mass and guarantees that no energy escapes from the pellets and contributes to pellet dose. In the case of gadolinium-added dosemeters the system is modelled through a sequence of LFM and gadolinium oxide layers. This requires that the neutron interactions happen more frequently inside the gadolinium layers and only some of the secondary particles released can reach the lithium formate layers and contribute to the energy released in them. Therefore, in this last case even though gadolinium has a larger cross section for neutron capture, the total energy released inside the sensitive layers of the dosemeters added with gadolinium oxide is smaller than that due to the presence of ^6Li in simple LFM dosemeters. Moreover, an increase of the gadolinium oxide content involves a reduction of the lithium formate inside the pellets, and this justifies the decrease of the absorbed dose with

Gd_2O_3 content inside the pellets. Also, in this case of Gd addition the absorbed dose inside the LFM pellet decreases as the water layer becomes thicker and therefore the energy released decreases with increase in the depth the pellets are placed at (see Figure 3). Furthermore, the energy released decreases with increasing the average energy of the neutron beams (data not shown). The absorbed dose is decreased to about 40% of its maximum value for Gd_2O_3 concentration of 75% for 'Spectrum B' neutron beam and to about 50% of its maximum value for Gd_2O_3 concentration of 75% for 'Spectrum C' neutron beam.

These MC results allow to conclude that the addition of gadolinium oxide could not improve significantly the neutron sensitivity of lithium formate pellets, whereas the increment or ^6Li content inside the sample could be more effective in improving the EPR response of lithium format to neutron beams. Experimental activity will be performed in future to investigate the actual dependence of EPR response of lithium formate after ^6Li or Gd addition.

Conclusions

In this work, analyses of the energy released for unit mass in lithium formate dosemeters exposed to neutron beams were carried out by means of Monte Carlo simulations having the target to predict the sensitivity enhancement achievable through ^6Li or Gd addition. As expected, the ^6Li addition involves an increase of neutron sensitivity because of its high ^6Li cross section for neutron capture and because of the charged secondary heavy particles being able to release energy inside the sensitive material layers. The maximum improvement was obtained for the beam mainly composed of thermal neutrons. The gadolinium addition is less effective than ^6Li in increasing the dose release inside the dosemeter layers. All results presented suggest that the ^6Li is preferable for improving neutron sensitivity of lithium formate pellets for dosimetric applications in NCT which exploits epithermal neutron beams for treatment of deep tumours.

Acknowledgments

This research was partially supported by the Istituto Nazionale di Fisica Nucleare (INFN) under the Project titled 'Next Artificial Intelligence in medicine' (nextAIM) and by the 'Fondo di Finanziamento per la Ricerca di Ateneo 2018/2021' provided by the University of Palermo.

References

[1] Barth, R F et al. Current status of boron neutron capture therapy of high grade gliomas and recurrent head and neck cancer. Radiat. Oncol. 7(1), 146 (2012).

[2] Suzuki, M Boron neutron capture therapy (bnct): A unique role in radiotherapy with a view to entering the accelerator-based bnct era. Int. J. Clin. Oncol. 25(1), 43–50 (2020).

[3] Porra, L, Seppälä, T, Wendland, L, Revitzer, H, Joensuu, H, Eide, P, Koivunoro, H, Smick, N, Smick, T and Tenhunen, M Accelerator-based boron neutron capture therapy facility at the helsinki university hospital. Acta Oncol. 61(2), 269–273 (2022).

[4] Sato, H, Nakajima, E, Gotanda, R, Endo, S, Suda, M, Hamano, T and Hoshi, M Experimental determination of the epithermal neutron sensitivity of a new ionization chamber. Physica Medica 32, 298 (2016).

[5] McGregor, D S and Shultis, J K Reporting detection efficiency for semiconductor neutron detectors: A need for a standard, Nuclear Instruments and Methods in Physics Research Section A: Accelerators,

Spectrometers, Detectors and Associated Equipment. 632(1), 167–174 (2011).

[6] Bell, Z W and Burger, A Semiconductor radiation detector. US Patent 7, 687,780 (2010).

[7] Triolo, A, Brai, M, Marrale, M, Gennaro, G and Bartolotta, A Study of the glow curves of TLD exposed to thermal neutrons. Radiat. Prot. Dosim. 126(1–4), 333–336 (2007).

[8] Triolo, A, Marrale, M and Brai, M Neutron-gamma mixed field measurements by means of MCP-TLD600 dosimeter pair. Nucl. Instrum. Methods Phys. Res., Sect. B 264(1), 183–188 (2007).

[9] Oliveira, L C, Yukihara, E G and Baffa, O MgO: Li, Ce, Sm as a high-sensitivity material for Optically Stimulated Luminescence dosimetry. Sci. Rep. 6, 1–12 (2016).

[10] Oliveira, L C and Baffa, O A new luminescent material based on CaB_6O_10:Pb to detect radiation. J. Lumin. 181, 171–178 (2017).

[11] Marrale, M, Longo, A, Bartolotta, A, D'Oca, M and Brai, M Preliminary application of thermoluminescence and single aliquot regeneration method for dose reconstruction in soda lime glass. Nucl. Instrum. Methods Phys. Res., Sect. B 297, 58–63 (2013).

[12] Lima, H R B R, Nascimento, D S and de Souza, S O Production and characterization of spodumene dosimetric pellets by prepared by pechini and proteic sol–gel route. Radiat. Meas. 71, 122–126 (2014).

[13] Marini, A, Valença, J V, Oliveira, R A, Souza, S O, Ciolini, R and d'Errico, F Production and characterization of H_3BO_3–Li_2CO_3–K_2CO_3– MgO glass for dosimetry. Radiat. Phys. Chem. 116, 92–94 (2015).

[14] Lima, H R B R, Nascimento, D S, Sussuchi, E M, d'Errico, F and de Souza, S O Synthesis of MgB_4O_7 and $Li_2B_4O_7$ crystals by proteic sol–gel and Pechini methods. J. Sol-Gel Sci. Technol. , 1–9 (2016).

[15] Bortolussi, S et al. Neutron flux and gamma dose measurement in the bnct irradiation facility at the triga reactor of the university of pavia. Nucl. Instrum. Methods Phys. Res., Sect. B 414, 113–120 (2018).

[16] Marrale, M et al. Correlation between ferrous ammonium sulfate concentration, sensitivity and stability of Fricke gel dosimeters exposed to clinical X-ray beams. Nucl. Instrum. Methods Phys. Res., Sect. B 335, 54–60 (2014).

[17] T Marques, M Schwarcke, C Garrido, V Zucolot, O Baffa, P Nicolucci, *Gel dosimetry analysis of gold nanoparticle application in kilovoltage radiation therapy*, in: Journal of Physics: Conference Series, 250, IOP Publishing, 2010, 012084.

[18] Marrale, M, Brai, M, Longo, A, Gallo, S, Tomarchio, E, Tranchina, L, Gagliardo, C et al. NMR relaxometry measurements of Fricke gel dosimeters exposed to neutrons. Radiat. Phys. Chem. 104, 424–428 (2014).

[19] Pavoni, J, Pike, T, Snow, J, DeWerd, L and Baffa, O Tomotherapy dose distribution verification using MAGIC-f polymer gel dosimetry. Med. Phys. 39(5), 2877–2884 (2012).

[20] Marrale, M, Collura, G, Gallo, S, Nici, S, Tranchina, L, Abbate, B F, Marineo, S, Caracappa, S and d'Errico, F Analysis of spatial diffusion of ferric ions in PVA-GTA gel dosimeters analyzed via magnetic resonance imaging. Nucl. Instrum. Methods Phys. Res., Sect. B 396, 50–55 (2017).

[21] Ciesielski, B and Wielopolski, L *Application of fricke dosimetry for bnct*. In: Advances in Neutron Capture Therapy. (Springer) pp. 53–57 (1993).

[22] Collura, G, Gallo, S, Tranchina, L, Abbate, B F, Bartolotta, A, d'Errico, F and Marrale, M Analysis of the response of pva-gta fricke-gel dosimeters with clinical magnetic resonance imaging. Nucl. Instrum. Methods Phys. Res., Sect. B 414, 146–153 (2018).

[23] Seco, J, Clasie, B and Partridge, M Review on the characteristics of radiation detectors for dosimetry

and imaging. Phys. Med. Biol. 59(20), R303 (2014).

[24] Regulla, D F From dating to biophysics–20 years of progress in applied esr spectroscopy. Appl. Radiat. Isot. 52(5), 1023–1030 (2000).

[25] Regulla, D F Esr spectrometry: a future-oriented tool for dosimetry and dating. Appl. Radiat. Isot. 62(2), 117–127 (2005).

[26] Ciesielski, B, Schultka, K, Kobierska, A, Nowak, R and Peimel-Stuglik, Z In vivo alanine/epr dosimetry in daily clinical practice: a feasibility study, International Journal of Radiation Oncology* Biology*. Physics 56(3), 899–905 (2003).

[27] Anton, M, Kapsch, R-P, Krystek, M and Renner, F Response of the alanine/ESR dosimetry system to MV x-rays relative to 60Co radiation. Phys. Med. Biol. 53(10), 2753 (2008).

[28] Baffa, O and Kinoshita, A Clinical applications of alanine/electron spin resonance dosimetry. Radiat. Environ. Biophys. 53(2), 233–240 (2014).

[29] Marrale, M, Carlino, A, Gallo, S, Longo, A, Panzeca, S, Bolsi, A, Hrbacek, J and Lomax, T EPR/alanine dosimetry for two therapeutic proton beams. Nucl. Instrum. Methods Phys. Res., Sect. B 368, 96–102 (2016).

[30] Garcia, T and Dolo, J-M Study of the influence of grain size on the ESR angular response in alanine radicals. Radiat. Meas. 42(6), 1207–1212 (2007).

[31] Brai, M, Gennaro, G, Marrale, M, Bartolotta, A and D'Oca, M ESR response to γ-rays of alanine pellets containing $B(OH)_3$ or Gd_2O_3. Appl. Radiat. Isot. 65(4), 435–439 (2007).

[32] Malinen, E, Heydari, M Z, Sagstuen, E and Hole, E O Alanine radicals, part 3: Properties of the components contributing to the epr spectrum of x-irradiated alanine dosimeters. Radiat. Res. 159(1), 23–32 (2003).

[33] Anton, M and Büermann, L Relative response of the alanine dosimeter to medium energy X-rays. Phys. Med. Biol. 60(15), 6113 (2015).

[34] Marrale, M, Brai, M, Gennaro, G, Triolo, A, Bartolotta, A, D'Oca, M and Rosi, G Alanine blends for ESR measurements of thermal neutron fluence in a mixed radiation field. Radiat. Prot. Dosim. 126(1–4), 631–635 (2007).

[35] Guidelli, E J, Ramos, A P, Zaniquelli, M E D, Nicolucci, P and Baffa, O Synthesis and characterization of gold/alanine nanocomposites with potential properties for medical application as radiation sensors. ACS Appl. Mater. Interfaces 4(11), 5844–5851 (2012).

[36] Guidelli, E J and Baffa, O Influence of photon beam energy on the dose enhancement factor caused by gold and silver nanoparticles: An experimental approach. Med. Phys. 41(3) (2014).

[37] Schultka, K, Ciesielski, B, Serkies, K, Sawicki, T, Tarnawska, Z and Jassem, J Epr/alanine dosimetry in ldr brachytherapy–a feasibility study. Radiat. Prot. Dosim. 120(1–4), 171–175 (2006).

[38] Schmitz, T et al. The alanine detector in BNCT dosimetry: Dose response in thermal and epithermal neutron fields. Med. Phys. 42(1), 400–411 (2015).

[39] Marrale, M, Schmitz, T, Gallo, S, Hampel, G, Longo, A, Panzeca, S and Tranchina, L Comparison of EPR response of alanine and Gd_2O_3alanine dosimeters exposed to TRIGA Mainz reactor. Appl. Radiat. Isot. 106, 116–120 (2015).

[40] Schmitz, T et al. Dose calculation in biological samples in a mixed neutron-gamma field at the triga reactor of the university of mainz. Acta Oncol. 49(7), 1165–1169 (2010).

[41] Marrale, M, Longo, A, Russo, G, Casarino, C, Candiano, G, Gallo, S, Carlino, A and Brai, M Dosimetry

for electron Intra-Operative RadioTherapy: Comparison of output factors obtained through alanine/EPR pellets, ionization chamber and Monte Carlo-GEANT4 simulations for IORT mobile dedicate accelerator. Nucl. Instrum. Methods Phys. Res., Sect. B 358, 52–58 (2015).

[42] Marrale, M, Longo, A, Span, M, Bartolotta, A, D'Oca, M and Brai, M Sensitivity of alanine dosimeters with gadolinium exposed to 6 MV photons at clinical doses. Radiat. Res. 176(6), 821–826 (2011).

[43] Marrale, M, Abbene, L, d'Errico, F, Gallo, S, Longo, A, Panzeca, S, Tana, L, Tranchina, L and Principato, F Characterization of the ESR response of alanine dosimeters to low-energy Cu-target X-tube photons. In Press on Radiation Measurements 106, 200–204 (2017).

[44] Lund, A, Olsson, S, Bonora, M, Lund, E and Gustafsson, H New materials for ESR dosimetry. Spectrochim. Acta A Mol. Biomol. Spectrosc. 58(6), 1301–1311 (2002).

[45] Marrale, M, Brai, M, Triolo, A, Bartolotta, A and D'Oca, M Power saturation of ESR signal in ammonium tartrate exposed to ^{60}Co γ-ray photons, electrons and protons. Radiat. Res. 166(5), 802–809 (2006).

[46] Marrale, M, Brai, M, Barbon, A and Brustolon, M Analysis of the spatial distribution of free radicals in ammonium tartrate by pulse EPR techniques. Radiat. Res. 171(3), 349–359 (2009).

[47] Maghraby, A, Mansour, A and Tarek, E Taurine for EPR dosimetry. Radiat. Environ. Biophys. 51(3), 255–261 (2012).

[48] Tuner, H and Kayıkçı, M Dosimetric and kinetic investigations of γ-irradiated sodium tartrate dihydrate. Radiat. Environ. Biophys. 51(1), 61–67 (2012).

[49] Lelie, S, Hole, E, Duchateau, M, Schroeyers, W, Schreurs, S and Verellen, D The investigation of lithium formate hydrate, sodium dithionate and N-methyl taurine as clinical EPR dosimeters. Radiat. Meas. 59, 218–224 (2013).

[50] Alzimami, K, Maghraby, A M and Bradley, D Comparative study of some new EPR dosimeters. Radiat. Phys. Chem. 95, 109–112 (2014).

[51] Brai, M, Marrale, M, Gennaro, G, Bartolotta, A, D'Oca, M and Rosi, G Improvement of ESR dosimetry for thermal neutron beams through the addition of gadolinium. Phys. Med. Biol. 52(17), 5219–5230 (2007).

[52] Marrale, M, Basile, S, Brai, M and Longo, A Monte Carlo simulation of the response of ESR dosimeters added with gadolinium exposed to thermal, epithermal and fast neutrons. Appl. Radiat. Isot. 67(7–8 SUPPL), S186–S189 (2009).

[53] Marrale, M, Brai, M, Gennaro, G, Triolo, A and Bartolotta, A Improvement of the LET sensitivity in ESR dosimetry for γ-photons and thermal neutrons through gadolinium addition. Radiat. Meas. 42(6–7), 1217–1221 (2007).

[54] Marrale, M, Gennaro, G, Brai, M, Basile, S, Bartolotta, A and D'Oca, M Exposure of Gd_2O_3-alanine and Gd_2O_3-ammonium tartrate ESR dosimeters to thermal neutrons: Experiments and Monte Carlo simulations. Radiat. Meas. 43(2–6), 471–475 (2008).

[55] Marrale, M, Brai, M, Gennaro, G, Bartolotta, A and D'Oca, M The effect of gadolinium on the ESR response of alanine and ammonium tartrate exposed to thermal neutrons. Radiat. Res. 169(2), 232–239 (2008).

[56] Brai, M, Gennaro, G, Marrale, M, Tranchina, L, Bartolotta, A and D'Oca, M ESR response to ^{60}Co-rays of ammonium tartrate pellets using Gd_2O_3 as additive. Radiat. Meas. 42(2), 225–231 (2007).

[57] Marrale, M, Brai, M, Longo, A, Panzeca, S, Tranchina, L, Tomarchio, E, Parlato, A, Buttafava, A and Dondi, D Neutron esr dosimetry through ammonium tartrate with low Gd content. Radiat. Prot. Dosim.

159(1–4), 233–236 (2014).

[58] Marrale, M, Longo, A, Brai, M, Barbon, A and Brustolon, M Discrimination of Radiation Quality Through Second Harmonic Out-of-Phase cw-ESR Detection. Radiat. Res. 181(2), 184–192 (2014).

[59] Rushdi, M, Abdel-Fattah, A and Soliman, Y Radiation-induced defects in strontium carbonate rod for EPR dosimetry applications. Radiat. Phys. Chem. 131, 1–6 (2017).

[60] Hoseininaveh, M and Ranjbar, A ESR response of CFQ–Gd_2O_3 dosimeters to a mixed neutron–gamma field: Monte Carlo simulation. Appl. Radiat. Isot. 105, 238–243 (2015).

[61] Ranjbar, A, Durrani, S and Randle, K Electron spin resonance and thermoluminescence in powder form of clear fused quartz: Effects of grinding. Radiat. Meas. 30(1), 73–81 (1999).

[62] Ranjbar, A, Aliabadi, R, Amraei, R, Tabasi, M and Mirjalily, G ESR response of bulk samples of clear fused quartz (CFQ) material to high doses from 10 MeV electrons: Its possible application for radiation processing and medical sterilization. Appl. Radiat. Isot. 67(6), 1023–1026 (2009).

[63] Gustafsson, H, Danilczuk, M, Sastry, M, Lund, A and Lund, E Enhanced sensitivity of lithium dithionates doped with rhodium and nickel for EPR dosimetry. Spectrochim. Acta A Mol. Biomol. Spectrosc. 62(1), 614–620 (2005).

[64] Marrale, M, Gallo, S, Longo, A, Panzeca, S, Parlato, A, Buttafava, A, Dondi, D and Zeffiro, A Study of the response of phenol compounds exposed to thermal neutrons beams for Electron Paramagnetic Resonance dosimetry. Radiat. Meas. 75, 15–20 (2015).

[65] Marrale, M, Longo, A, Panzeca, S, Gallo, S, Principato, F, Tomarchio, E, Parlato, A, Buttafava, A, Dondi, D and Zeffiro, A ESR response of phenol compounds for dosimetry of gamma photon beams. Nucl. Instrum. Methods Phys. Res., Sect. B 339, 15–19 (2014).

[66] Gallo, S, Panzeca, S, Longo, A, Altieri, S, Bentivoglio, A, Dondi, D, Marconi, R, Protti, N, Zeffiro, A and Marrale, M Testing and linearity calibration of films of phenol compounds exposed to thermal neutron field for EPR dosimetry. Appl. Radiat. Isot. 106, 129–133 (2015).

[67] Gallo, S et al. Characterization of phenolic pellets for ESR dosimetry in photon beam radiotherapy. Biophysik 56, 471–480 (2017).

[68] Gallo, S, Iacoviello, G, Bartolotta, A, Dondi, D, Panzeca, S and Marrale, M ESR dosimeter material properties of phenols compound exposed to radiotherapeutic electron beams. Nucl. Instrum. Methods Phys. Res., Sect. B 407, 110–117 (2017).

[69] Marrale, M et al. EPR/alanine pellets with low Gd content for neutron dosimetry. Radiat. Prot. Dosim. 161(1–4), 383–386 (2014).

[70] Vestad, T A, Malinen, E, Lund, A, Hole, E O and Sagstuen, E Epr dosimetric properties of formates. Appl. Radiat. Isot. 59(2–3), 181–188 (2003).

[71] Gustafsson, H, Lund, E and Olsson, S Lithium formate EPR dosimetry for verifications of planned dose distributions prior to intensity-modulated radiation therapy. Phys. Med. Biol. 53(17), 4667 (2008).

[72] Lund, E, Gustafsson, H, Danilczuk, M, Sastry, M, Lund, A, Vestad, T, Malinen, E, Hole, E and Sagstuen, E Formates and dithionates: sensitive EPR-dosimeter materials for radiation therapy. Appl. Radiat. Isot. 62(2), 317–324 (2005).

[73] Malinen, E, Waldeland, E, Hole, E O and Sagstuen, E Let effects following neutron irradiation of lithium formate epr dosimeters. Spectrochim. Acta A Mol. Biomol. Spectrosc. 63(4), 861–869 (2006).

[74] Adolfsson, E, Karlsson, M, Carlsson, G A, Tedgren, Å C, Lund, E, Olsson, S and Gustafsson, H Investigation of signal fading in lithium formate epr dosimeters using a new sensitive method. Phys.

Med. Biol. 57(8), 2209 (2012).

[75] Höfel, S, Stehle, M, Zwicker, F, Fix, M K and Drescher, M A practical epr dosimetry system for routine use in radiotherapy: uncertainty analysis of lithium formate dosimeters at the therapeutic dose level. Phys. Med. Biol. 66(4), 045005 (2021).

[76] Adolfsson, E, Gustafsson, H, Lund, E, Carlsson, G A, Olsson, S and Tedgren, Å C A system for remote dosimetry audit of 3d-crt, imrt and vmat based on lithium formate dosimetry. Radiother. Oncol. 113(2), 279–282(2014).

[77] Krivokapic, A, Sanderud, A, Aalbergsjø, S G, Hole, E O and Sagstuen, E Lithium formate for epr dosimetry (2): secondary radicals in x-´ irradiated crystals. Radiat. Res. 183(6), 675–683 (2015).

[78] Lund, E, Gustafsson, H, Danilczuk, M, Sastry, M and Lund, A Compounds of 6li and natural li for epr dosimetry in photon/neutron mixed radiation fields. Spectrochim. Acta A Mol. Biomol. Spectrosc. 60(6), 1319–1326 (2004).

[79] Briesmeister, J F et al. MCNPTM-A general Monte Carlo N-particle transport code. Tech. rep. (2000).

[80] Longo, A, Collura, G, Gallo, S, Bartolotta, A and Marrale, M Monte carlo simulation of energy absorbed in phenolic esr dosimeters added with gadolinium exposed to thermal, epithermal and fast neutrons. Nucl. Instrum. Methods Phys. Res., Sect. B 410, 21–28(2017).